Title

Strain-Release Pentafluorosulfanylation and Tetrafluoro(aryl)sulfanylation of [1.1.1]Propellane: Reactivity and Structural Insight**

Journal

Angewandte Chemie International Edition, 61(48)

ISSN

1433-7851

Authors

Kraemer, Yannick
Ghiazza, Clément
Ragan, Abbey N
et al.

Publication Date

2022-11-25

DOI

10.1002/anie.202211892

Peer reviewed

How to cite: *Angew. Chem. Int. Ed.* **2022,** *61,* e202211892
International Edition: doi.org/10.1002/anie.202211892
German Edition: doi.org/10.1002/ange.202211892

Propellanes

Strain-Release Pentafluorosulfanylation and Tetrafluoro(aryl)sulfanylation of [1.1.1]Propellane: Reactivity and Structural Insight**

Yannick Kraemer[+], Clément Ghiazza[+], Abbey N. Ragan, Shengyang Ni, Sigrid Lutz, Elizabeth K. Neumann, James C. Fettinger, Nils Nöthling, Richard Goddard, Josep Cornella, and Cody Ross Pitts**

Abstract: We leveraged the recent increase in synthetic accessibility of SF_5Cl and Ar–SF_4Cl compounds to combine chemistry of the SF_5 and SF_4Ar groups with strain-release functionalization. By effectively adding SF_5 and SF_4Ar radicals across [1.1.1]propellane, we accessed structurally unique bicyclopentanes, bearing two distinct elements of bioisosterism. Upon evaluating these "hybrid isostere" motifs in the solid state, we measured exceptionally short transannular distances; in one case, *the distance rivals the shortest nonbonding C···C contact reported to date.* This prompted SC-XRD and DFT analyses that support the notion that a donor-acceptor interaction involving the "wing" C–C bonds is playing an important role in stabilization. Thus, these heretofore unknown structures expand the palette for highly coveted three-dimensional fluorinated building blocks and provide insight to a more general effect observed in bicyclopentanes.

Introduction

The pentafluorosulfanyl (SF_5) group is situated on an exclusive list of fluorinated functional groups with documented utility that remain underemployed.[1] The reason for this dissonance is attributed to limited pentafluorosulfanylation methods and reagents, particularly with respect to introducing the SF_5 group to aliphatic frameworks.[2] For instance, SF_5Cl gas—one of the few reliable sources of SF_5 radicals with applications in $C(sp^3)$–SF_5 synthesis[3]—has been historically difficult to synthesize and handle,[4] thus preventing widespread adoption of the chemistry and impeding further innovation. This contrasts with the relative accessibility of its Ar–SF_4Cl congeners,[5] which are analogous sources of Ar–SF_4 radicals with applications in $C(sp^3)$–SF_4Ar synthesis.[6]

However, as part of a larger effort to make polyfluorinated groups more accessible in 2019,[7] one of us disclosed the first user-friendly, gas-reagent free synthesis of SF_5Cl in the patent literature through oxidative fluorination of S_8

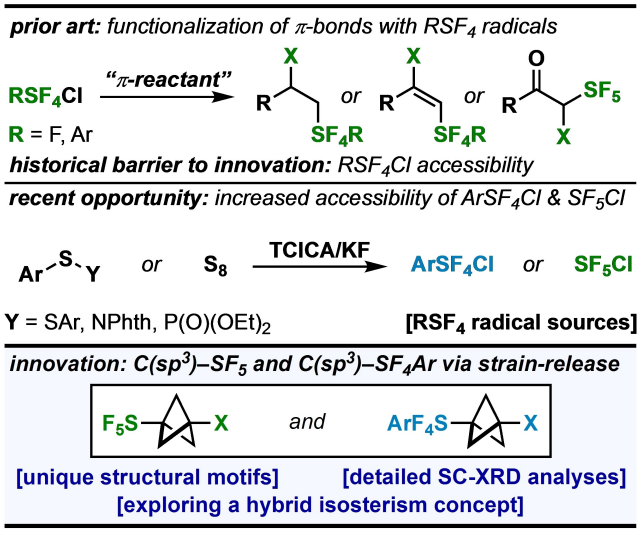

Figure 1. Strain-release pentafluoro- and tetrafluoro(aryl)sulfanylation in context. (Top panel) Known reactivity of SF_4R radicals and barrier to innovation. (Middle panel) Recent increased accessibility of key reagents. (Bottom panel) This work.

[*] Y. Kraemer,[+] A. N. Ragan, Prof. Dr. E. K. Neumann, Dr. J. C. Fettinger, Prof. Dr. C. R. Pitts
Department of Chemistry,
University of California, Davis
1 Shields Avenue, Davis, CA 95616 (USA)
E-mail: crpitts@ucdavis.edu

Dr. C. Ghiazza,[+] Dr. S. Ni, S. Lutz, Dr. N. Nöthling, Dr. R. Goddard, Prof. Dr. J. Cornella
Max-Planck-Institut für Kohlenforschung
Kaiser-Wilhelm-Platz 1, 45470 Mülheim an der Ruhr (Germany)
E-mail: cornella@kofo.mpg.de

[+] These authors contributed equally to this work.

[**] A previous version of this manuscript has been deposited on a preprint server (https://doi.org/10.26434/chemrxiv-2022-2qmq3).

using inexpensive trichloroisocyanuric acid (TCICA) and potassium fluoride.[8] In 2021, Qing and co-workers reported an optimized workup protocol for this TCICA/KF approach whereby SF_5Cl can be extracted directly into hexanes to produce a storable stock solution, *thus obviating the need to handle SF_5Cl as a gas.*[9] Together, these recent advancements not only enable the broader chemical community to synthesize their own SF_5Cl solution more safely, but facilitates the invention of pentafluorosulfanylation reactions and the study of heretofore unknown SF_5-containing motifs.[10]

To date, the known methods of forming $C(sp^3)$–SF_5 and $C(sp^3)$–SF_4Ar bonds from either SF_5 or Ar–SF_4 radicals involve formal addition to π-systems (Figure 1, *top*). Alternatively, with the key reagents more accessible (Figure 1, *middle*), we sought opportunities to add SF_5Cl and Ar–SF_4Cl compounds across other types of bonds such as the central bond in [1.1.1]propellane.[11] Conceptually, the result of combining SF_5 radical chemistry with strain-release functionalization[12] would enable investigation of the structural consequences of merging a bioisosteric replacement for phenyl groups or alkynes (i.e., bicyclopentane, or "BCP")[13] with a bioisosteric surrogate for trifluoromethyl or *tert*-butyl groups (i.e., SF_5).[14] Additionally, appending an Ar–SF_4 moiety with a BCP ring would provide access to another type of hybrid isostere that may be of interest in the design of materials, such as liquid crystals.[15]

Herein, we report a mild, radical pentafluorosulfanylation and tetrafluoro(aryl)sulfanylation of [1.1.1]propellane (Figure 1, *bottom*). Based on a detailed structural analysis of this unusual SF_5–BCP motif, we also found that the resulting transannular C···C distance in SF_5–BCP–Cl is one of the shortest allegedly nonbonding C···C distances reported in the CSD (see Supporting Information for search details). This prompted synthesis of a suite of tetrafluoro(aryl)sulfanyl derivatives and extensive single-crystal X-ray diffraction (SC-XRD) and NMR comparative analyses. Furthermore, the nature of the dramatic impact of the SF_5 group on the BCP ring scaffold was studied further using density functional theory (DFT).

Results and Discussion

We began our investigation by applying a well-established strategy to generate SF_5 radicals from SF_5Cl (i.e., using catalytic BEt_3/O_2) in the presence of [1.1.1]propellane (**1**).[16] The desired SF_5–BCP–Cl product (**2**) was observed by ^{19}F NMR in a promising 48% yield.[17] This prompted an optimization campaign that led to the discovery that irradiating SF_5Cl and **1** with white LEDs for 4 h would ultimately allow isolation of volatile **2** in 86% yield (Figure 2, *top left*).

Based on previous literature on both SF_5Cl and **1**, a radical chain propagation mechanism is most likely at play following initial formation of SF_5 radicals (see Supporting Information for calculated free energy profiles).[18] Control experiments indicate that SF_5Cl does not undergo decomposition under irradiation with white LEDs in the absence of **1**, suggesting **1** is involved in the initiation step.[19] It is

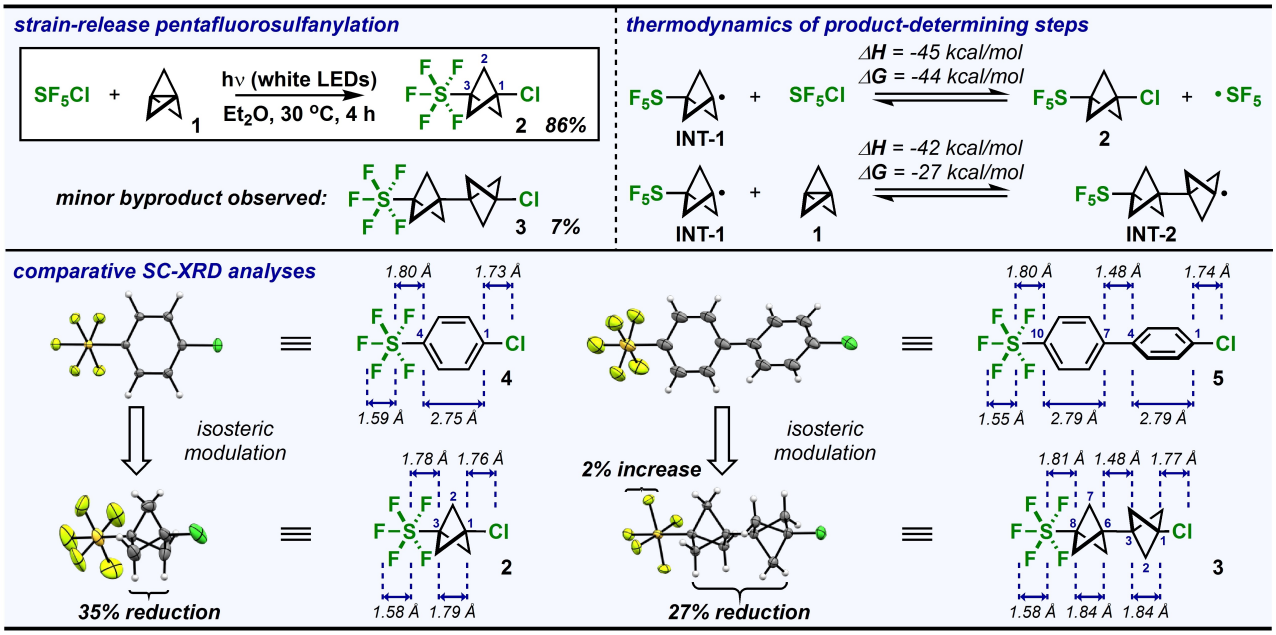

Figure 2. (Top left panel) Major product **2** (and minor byproduct **3**) observed under optimized pentafluorosulfanylation conditions, using 1.5 equiv SF_5Cl and 1.0 equiv **1**. Isolated yields reported. (Top right panel) Thermodynamic parameters associated with the product-determining steps, calculated at ωB97XD/6-311++G** using the default Et_2O solvent continuum. (Bottom panel) Structural differences in the linear array of atoms upon net replacement of benzene rings in **4** and **5** with bicyclopentane (BCP) rings to make "hybrid" SF_5–BCP isosteres **2** and **3**. Structures determined by single-crystal X-ray diffraction (displacement ellipsoids depicted at 50% probability). Only non-disordered parts are shown for clarity.

plausible that SF_5 radicals are formed initially through visible light-excitation of an electron donor-acceptor complex between SF_5Cl and **1** and then propagate a radical chain reaction, similar to the mechanism proposed by Paquin and co-workers.[3b] Additionally, we isolated a minor byproduct (**3**) in 7 % yield that incorporates two bicyclopentane motifs; similar types of dimerization products (i.e., "[2]staffanes") have been observed previously in radical chain processes involving **1**.[20] The difference in free energies calculated at ωB97XD/6-311++G** (using the default Et_2O solvent continuum) for the product determining steps are also consistent with our observed selectivity, as the path from putative **INT-1** to **2** is 17 kcal mol^{-1} more exergonic than to **INT-2** (Figure 2, *top right*).

After much effort, we also managed to grow single crystals of **2** suitable for X-ray diffraction to examine the SF_5–BCP motif in the solid state at 100 K (Figure 2, *bottom*). The most striking feature is the exceptionally short transannular $C_1\cdots C_3$ distance of 1.789(6) Å (libration corrected value: 1.800 Å).[21] It is notably within error of the transannular $C_1\cdots C_3$ distance reported for Adcock and co-workers' pyridinium-substituted bicyclopentane—1.80(2) Å—which they claimed at the time was, "*not only the shortest nonbonding contact for bicyclo[1.1.1]pentanes but also for any known organic compound.*"[22] To put it in perspective, the transannular distance in **2** is significantly shorter than in an unsubstituted [1.1.1]bicyclopentane (with a transannular distance of ≈1.85–1.87 Å)[23] and is approaching that of one of the longest C–C bonds reported (i.e., 1.780(7) Å).[24]

To put the structural features of the linear array of atoms about the C_1-C_3 axis of **2** into context, we obtained SC-XRD data for SF_5–Ph–Cl (**4**). This allowed us to assess the consequences of Ph→BCP isosteric replacement in the presence of an SF_5 group (Figure 2, *bottom*). While maintaining a relatively linear central axis, the $C_1\cdots C_3$ transannular distance in **2** is attenuated by ≈35 % relative to the $C_1\cdots C_4$ distance in **4** (2.745(1) Å). The C–S bond in **2** is marginally shorter than in **4** (1.779(4) Å[21] vs. 1.7952(6) Å, respectively), while the C–Cl bond in **2** is slightly longer than in **4** (1.759(5) Å[21] vs. 1.7302(6) Å, respectively). The equatorial fluorine (F_{eq}) atoms of the SF_5 group on both **2** and **4** sport average S–F_{eq} distances of ≈1.57–1.59 Å, and $\theta_{C3\text{-}S\text{-}Feq}$ for both **2** and **4** deviates only slightly from perpendicularity on average (i.e., ≈92.3° vs. ≈92.6°). We also noted that the axial S–F_{ax} bond length in **2** at 1.579(4) Å[21] is within range of **4** (1.5869(5) Å).

Additionally, we obtained SC-XRD data for the [2]staffane byproduct—SF_5–BCP–BCP–Cl (**3**)—to compare alongside **2** as well as the previously published structure of its SF_5–Ph–Ph–Cl congener, **5** (Figure 2, *bottom*).[25] In this case, both transannular C···C distances in the bicyclopentane rings of **3** (1.835(4) Å and 1.839(4) Å) are notably longer than that of **2**. Alternatively, the conduit C–C bonds connecting the ring structures in **3** and **5** are similar in length; this makes the composite effect of replacing both Ph rings in the biphenyl array with BCP rings a ≈27 % reduction in distance between the terminal carbon atoms. Also, similar to **2** vs. **4**, the C–Cl bond in **3** is longer than in **5**, and average S–F_{eq} distances are ≈1.58–1.60 Å in each case. However, the S–F_{ax} bond in **3** is ≈2 % longer than in **5**.

At this juncture, we envisioned that incorporation of an Ar–SF_4 moiety on the BCP ring instead of SF_5 would allow us to explore another concept in "hybrid isosterism," as the *trans*-substituted -SF_4- linear architecture has been entertained as a replacement for an alkyne (or even a BCP ring).[26] This would also prove advantageous for further crystallographic analyses, as modification of the aryl group allows us to examine effects of remote substitution on the BCP ring. Under identical conditions to the reaction of SF_5Cl with **1**, we discovered that Ar–SF_4Cl compounds can indeed be converted into the desired Ar–SF_4–BCP–Cl products, albeit in modest yields. Thus, the reaction conditions were re-optimized explicitly for Ar–SF_4Cl addition across **1**.[17] Note that, in this case, the reaction proceeds spontaneously in the dark at −45 °C. The propensity of Ar–SF_4Cl compounds to react more readily with **1** than SF_5Cl is consistent with the fact that the S–Cl bond has been determined to be weaker in Ar–SF_4Cl compounds (i.e., computed BDEs are on the order of 6–7 kcal mol^{-1} lower than the S–Cl BDE in SF_5Cl).[6a] It is also known that both **1**[27] and Ar–SF_4Cl compounds,[28] independently, can initiate radical chain propagations spontaneously in some cases in the absence of a designated radical initiator or other initiation source, such as light.

We then explored the scope of accessible arene- and heteroarene-containing compounds under optimized conditions (Figure 3, *top*). For one, Ar–SF_4Cl starting materials containing benzene rings—either unsubstituted or substituted with electron-withdrawing groups—provided the desired addition products **6**–**8** in good yields. Moreover, starting materials containing pyridine rings with various halogen (**9**–**11**), cyano (**12**), ester (**13**), trifluoromethyl (**14**), and nitro (**15**) substituents performed generally well under specified conditions. Additionally, the scope includes examples of pyrimidine-containing products, such as **16** and **17** - the latter formed in 97 % yield by ^{19}F NMR and isolated in 84 %. During these studies, we noted that pyridine- and pyrimidine-based products of all substitution patterns were *generally* less prone to decomposition during attempted purification than benzene-based products without a strong electron withdrawing substituent present (e.g., a nitro group), though we noted some exceptions (**6** and **7**). This phenomenon is in accord with what has been observed previously in compounds containing the Ar–SF_4 moiety,[6] and we have indicated a few examples of compounds in our Supporting Information where decomposition on silica gel (or basic alumina) was problematic, in contrast to the entries shown in Figure 3.

In the process of examining the reaction scope, we managed to obtain SC-XRD data on compounds **7**, **8**, **9**, and **17** (Figure 3, *bottom*). In this suite, the $C_1\cdots C_3$ transannular distances are still unusually short but all slightly longer than that of **2**,[21] decreasing in the order of: **8** (1.812(2) Å) ≈ **9** (1.8123(18) Å) > **7** (1.809(2) Å) > **17** (1.802(2) Å). The C_3–S bonds (ranging from 1.806(1) Å in **17** to 1.8119(12) Å in **9**) and the S–F_{eq} bonds (average distances of ≈1.62–1.64 Å in the series) are also both notably longer in these

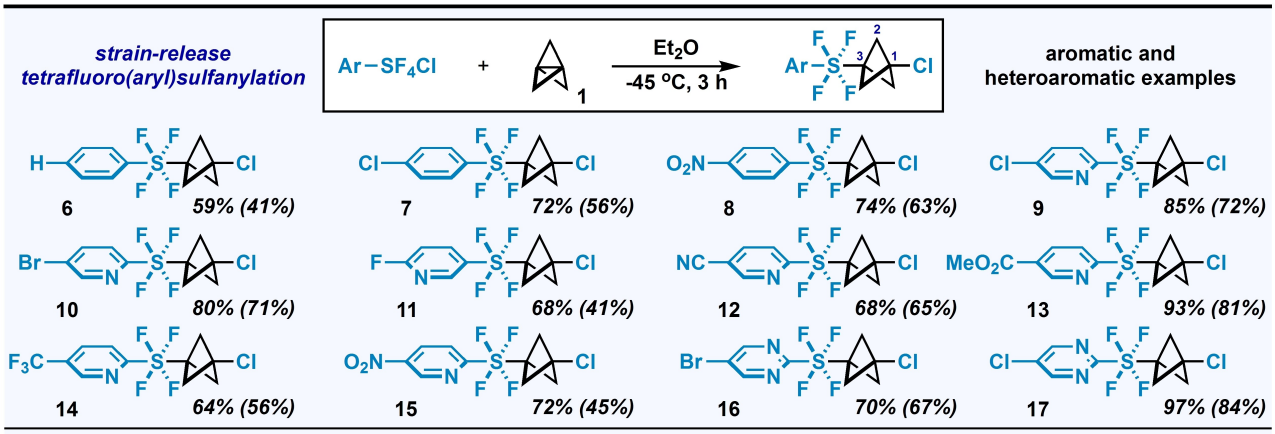

comparative SC-XRD and NMR analyses

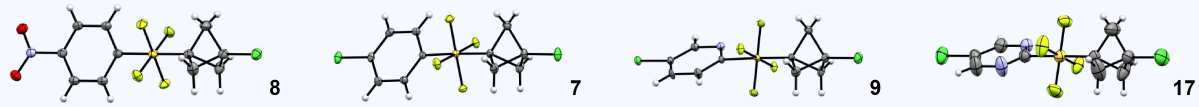

distances (Å) and angles				
C_1–C_3	1.812(2)	1.809(2)	1.8123(18)	1.802(2)
C_1–Cl	1.752(1)	1.766(1)	1.7648(14)	1.764(2)
S–C_3	1.808(1)	1.811(1)	1.8119(12)	1.806(1)
S–C_{Ar}	1.820(1)	1.817(1)	1.8386(13)	1.847(1)
S–F_{eq}	1.6219(9)-1.6319(7)	1.6200(7)-1.6336(7)	1.6213(6)-1.6371(6)	1.6109(8)-1.621(1)
C_3-S-F_{eq}	89.60(4)-90.78(5)°	88.10(4)-91.29(5)°	88.68(4)-91.21(3)°	89.62(6)-91.49(5)°
C_3-S-C_{Ar}	179.81(5)°	177.41(5)°	177.36(6)°	178.99(6)°
isotropic NMR shifts (ppm)				
C_3	68.6	68.9	67.8	67.0
C_{Ar}	163.6	158.2	167.6	171.1
F_{eq}	+55.9	+55.6	+46.5	+43.6

Figure 3. (Top panel) Reaction scope under optimized tetrafluoro(aryl)sulfanylation conditions, using 1.0 equiv $ArSF_4Cl$ and 1.2 equiv **1**. ^{19}F NMR yields are reported; isolated yields are in parentheses. (Bottom panel) Structural differences and select ^{13}C and ^{19}F NMR data associated with the linear array of atoms upon systematic alteration of electronic properties of the (hetero)arene. Structures determined by single-crystal X-ray diffraction (displacement ellipsoids depicted at 50% probability).

Ar–SF_4–BCP–Cl compounds than in **2**. The C_1–Cl bond length in these four compounds varies but is centered around that of **2**, ranging from 1.752(1) Å in **8** to 1.766(1) Å in **7**. Another noticeable difference is that the $\theta_{C3\text{-}S\text{-}Feq}$ in these Ar–SF_4–BCP–Cl compounds, on average, is closer to 90° than in **2**, where the equatorial fluorine atoms of the SF_5 group seem to pucker away from the BCP ring. This could be attributed to an increased repulsive interaction between the equatorial fluorine atoms and the BCP ring in **2**, as **2** exhibits a shorter C_3–S bond than the Ar–SF_4–BCP–Cl compounds.

A trend can be found in the linear array of atoms in the four Ar–SF_4–BCP–Cl compounds in Figure 3: the C_{Ar}–S bond lengths increase as the (hetero)arenes become increasingly electron deficient, i.e., in the order of **7** (1.817(1) Å) < **8** (1.820(1) Å) < **9** (1.8386(13) Å) < **17** (1.847(1) Å). This type of trend has been observed previously in other compounds containing an Ar–SF_4 motif and is associated with an increase in ionic character in the C_{Ar}–S bond.[6,29] The dramatic "downfield" shift in ^{13}C NMR shift of the *ipso* carbon atom (C_{Ar}) from **7** to **17** is also consistent with this idea (note that the cross-ring C_3 atom ^{13}C shift is less impacted by remote arene functionalization but experiences the opposite trend).

Additionally, we managed to obtain and analyze SC-XRD data for meta-stable Ar–SF_4Cl compounds **18** and **19** —the starting materials for **8** and **15**, respectively (Figure 4). When compared alongside the only other two Ar–SF_4Cl compounds reported in the solid state,[24] they seem to also follow this trend of increasing S–C_{Ar} distance with electron-withdrawing effect of the arene (concomitant with a decrease in S–Cl distance).

Finally, we sought more insight as to *why* the C_1···C_3 contact is so short in the structures included in this study, especially in the instance of **2**. Broadly, the tendency for σ-electron withdrawing groups to decrease the C_1···C_3 distance in BCP rings has been established in the literature and is often attributed to some type of through-space interaction involving the linear arrangement of atoms about the C_1–C_3 axis (e.g., both an attractive "percaudal" interaction[30] and a decrease in e^-–e^- repulsion between rear orbital lobes contribute to this effect).[11a,31] It has also come to light that a form of hyperconjugation involving the "wing" C–C bonds may contribute significantly to stabilization (e.g., in studies

SC-XRD analyses of tetrafluoro(aryl)sulfanyl chlorides

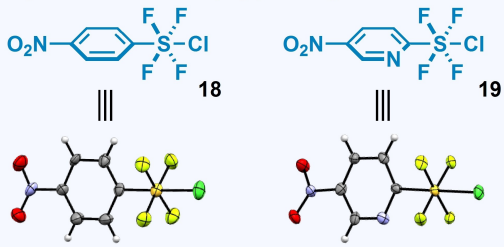

distances (Å) and angles		
S–Cl	2.0807(6), 2.0846(7)	2.066(3)
S–C_{Ar}	1.816(1), 1.816(2)	1.83(1)
S–F_{eq}	1.594(1)-1.606(1)	1.589(7)-1.599(6)
C_{Ar}-S-F_{eq}	91.23(7)-91.80(7)°	90.8(4)-91.9(4)°
C_{Ar}-S-Cl	179.42(6), 179.56(6)°	179.3(3)°

Figure 4. Structures of Ar–SF_4Cl starting materials determined by single-crystal X-ray diffraction (displacement ellipsoids depicted at 50% probability). The unit cell for **18** contains two symmetry-independent moieties (only one shown).

pertaining to the bicyclo[1.1.1]pent-1-yl cation, among others).[32,33] To study this systematically, we performed geometry optimization and natural bond orbital (NBO) second-order perturbation analysis of SF_5–BCP–Cl (**2**) at ωB97XD/cc-pVQZ, as well as BCP (**20**), SF_5–BCP–H (**21**), and Cl–BCP–H (**22**) for comparisons (Figure 5, *top left*).[34]

The trend in computed $C_1\cdots C_3$ distances (as well as $\theta_{C1\text{-}C2\text{-}C3}$ angles) is as expected, following the increase in electron-withdrawing effect: **2** > **22** ≈ **21** > **20**. The Wiberg bond index between C_1 and C_3 also seems to follow a similar trend, increasing from 0.035 in **20** to 0.085 in **2** (while this trend is noteworthy, these values are too small to argue incipient bond formation).[35] Additionally, by NBO analysis, *the wing C–C bonds contribute a far greater two-electron stabilization energy* via *a side-on interaction than donor-acceptor interactions in the linear array* (Figure 5, *top left*). While computed NBO energies should be carefully considered as only an "upper bound" for actual stabilization energies due to overestimation of electron delocalization effects,[32] the computed wing stabilization energies are over an order of magnitude larger than the percaudal interaction energies in each case. Moreover, the stabilization energies increase when wing C–C bonds are situated across the ring from electron-withdrawing substituents (**21**, **22**, and **2**), consistent with increased orbital overlap.[36] Representative depictions of these key donor-acceptor interactions in **2**, resembling an agostic-like donation from the wing C–C σ-bond to the $\sigma^*_{C\text{-}EWG}$ orbital, can be found in Figure 6.

Intuitively, a simplified resonance-like depiction of this type of wing interaction (Figure 5, *top right*) accounts for more "bonding character" between C_1 and C_3, and it also suggests there should be a lengthening in the C_3–C_2 bond opposite the EWG relative to the C_1–C_2 bond.[37] For experimental support, we turned to the X-ray structure of compound **3**. Here, we see a break in symmetry in both BCP rings and elongation of all wing bonds opposite the EWG's versus the adjacent ones (i.e., d(C_3–C_2) and d(C_6–C_7) ≈1.56 Å vs. d(C_1–C_2) and d(C_8–C_7) ≈1.54 Å). While the depiction also suggests elongation of the C–EWG bond, this

calculated donor-acceptor orbital interactions

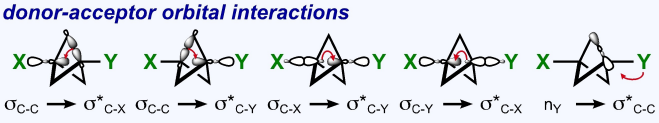

	X	Y	ΔE_{ij}[a]	ΔE_{ij}[a]	ΔE_{ij}	ΔE_{ij}	ΔE_{ij}[b]
20	H	H	8.60	8.60	0.58	0.58	-
21	SF_5	H	13.18	8.58	0.74	0.38	-
22	H	Cl	8.82	18.72	0.61	0.42	10.44
2	SF_5	Cl	**12.60**	**17.39**	0.82	0.25	**11.03**

[a]Average value from 3 "wing" C-C bonds for $\sigma_{C\text{-}C}$ or $\sigma^*_{C\text{-}C}$. [b]Average value from 3 lone pairs for n_{Cl}.

structural manifestation of wing interaction

prediction (DFT):

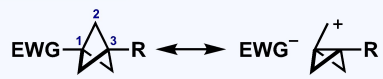

∴ *reduced* $C_1\cdots C_3$ *distance and* $d(C_3\text{-}C_2) > d(C_1\text{-}C_2)$

consistent observation (SC-XRD):

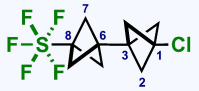

$d(C_6\text{-}C_7) > d(C_8\text{-}C_7)$ $d(C_3\text{-}C_2) > d(C_1\text{-}C_2)$

composite effect of two EWG's: short $C_1\cdots C_3$ distance and less disparity in C_1–C_2 and C_3–C_2 distances

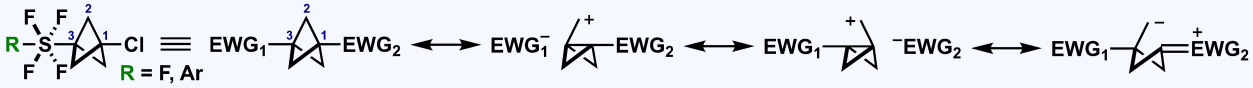

	2	**7**	**8**	**9**	**17**
C_1–C_2	1.468(8)-1.609(10)	1.545(2)-1.552(2)	1.539(2)-1.549(2)	1.545(2)-1.5476(13)	1.532(2)-1.537(2)
C_3–C_2	1.533(8)-1.553(9)	1.547(2)-1.549(2)	1.542(2)-1.549(2)	1.5480(13)-1.5494(18)	1.533(2)-1.538(2)
C_1-C_2-C_3	68.9(4)-73.2(4)°	71.39(8)-71.63(8)°	71.61(9)-71.98(9)°	71.67(7)-71.70(9)°	71.8(1)-72.0(1)°

Figure 5. (Top left panel) Comparative analysis of significant donor-acceptor interactions. Geometry optimizations and NBO analyses conducted at ωB97XD/cc-pVQZ. ΔE_{ij} (in kcal mol^{-1}) is the two-electron stabilization energy associated with delocalization between donor (i) and acceptor (j) NBOs. (Top right panel) Observations in SC-XRD data of **3** consistent with predicted structural effects. (Bottom panel) Depiction of composite effects from donor-acceptor interactions consistent with observed short $C_1\cdots C_3$ contacts and less disparity in wing C–C distances in SC-XRD data for **2**,[21] **7**–**9**, and **17**. Distances reported in angstroms (Å).

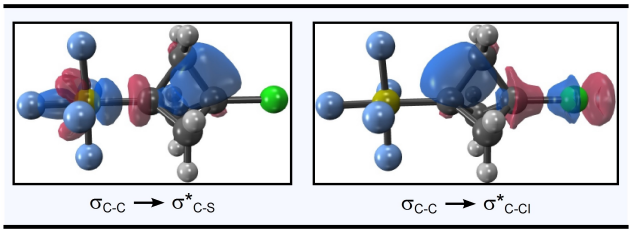

Figure 6. Molecular orbital depictions of donor-acceptor interactions involving wing C–C bonds in compound **2**. NBOs were generated at ωB97XD/cc-pVQZ.

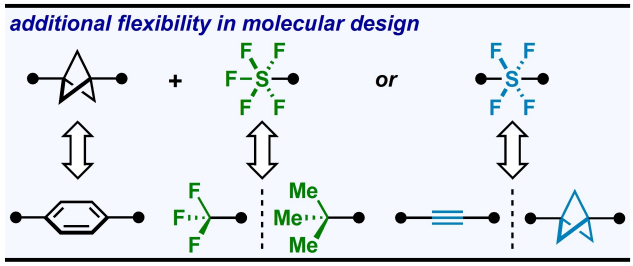

Figure 7. Highlighting the mix-and-match design potential associated with hybrid isosteres.

is complicated for the C–Cl bond, as the stabilization energy derived from Cl lone-pair donation into wing σ^*_{C-C} orbitals is not negligible, and this would conceptually manifest in shortening of the bond (i.e., effects may cancel each other out). However, in the case of the SF_5 group (devoid of a lone pair), the predicted structural manifestation of this interaction is clearer, as the C–S bond in **3** is longer than in **2** by ≈1.5 % (Figure 2, *bottom*).

It is also apparent that the $C_1\cdots C_3$ distance in the X-ray structure of **3** is approximately equal to the $C_6\cdots C_8$ distance (≈1.84 Å), both of which are shorter than the $C_1\cdots C_3$ distance in unsubstituted [1.1.1]bicyclopentane.[23] This indicates that a Cl atom and an SF_5 group have a similar composite effect on shortening the transannular distance in a BCP ring. One can attribute this in large part to the strong electron withdrawing effects of these substituents through the σ-framework.[38]

Lastly, when the bicyclopentane ring is substituted with two σ-EWG's, a unifying depiction of dominant donor-acceptor interactions by NBO analysis (Figure 5, *bottom*) also accounts for the further decrease in $C_1\cdots C_3$ distance and would suggest that there are competing forces dictating bond elongation/contraction and charge distribution on the wings.[31b] Theoretically, these *push-pull* effects would not result in the same structural trends observed for compounds like **3**; in fact, this was found to be the case experimentally in structures **2**, **7**, **8**, **9**, and **17** (Figure 5, *bottom*).

Conclusion

This work was originally motivated by the methodological advancement of forging novel, tertiary $C(sp^3)$–SF_5 and $C(sp^3)$–SF_4Ar bonds through strain-release functionalization of [1.1.1]propellane. As SF_5–BCP and –SF_4–BCP motifs were recognized in this study as types of hybrid isosteres (for [CF_3/*t*-Bu + Ph] and [alkyne/BCP + Ph], respectively; see Figure 7), this prompted detailed SC-XRD studies that led to the discovery and additional investigations of short transannular C···C distances. Lastly, DFT calculations and previous literature support the notion that donor-acceptor interactions involving the wing C–C bonds in BCP rings play a significant role (alongside linear through-space interactions) in this shortening phenomenon. The theoretical model was corroborated by X-ray data,[39] whereby manifestations of these "wing donation" effects were observed in solid-state structures.

We believe these "hybrid isosteres" afford an unusual and subtle type of flexibility in molecular design that may prove useful (Figure 7). Following this critical proof of concept and detailed structural study, future work will pertain to installing SF_5–BCP and $ArSF_4$–BCP motifs onto more complex molecules and evaluating applications.

Acknowledgements

Y. K., A. N. R., J. C. F., and C. R. P. thank Wang-Yeuk Kong, Yusef Ahmed, Prof. Dean J. Tantillo, and Dr. Nils Trapp for helpful discussions, the UC Davis core NMR facility, and the National Science Foundation (CHE-1531193) for the Dual Source X-ray Diffractometer. Financial support for this work was provided by Max-Planck-Gesellschaft, Max-Planck-Institut für Kohlenforschung, Fonds der Chemischen Industrie (FCI-VCI) and Boehringer Ingelheim Foundation (Exploration Grant BIS), and the University of California, Davis. C. G. thanks the Alexander von Humboldt Stiftung for a Postdoctoral Fellowship. We especially thank Prof. Dr. A. Fürstner for generous support. Open Access funding enabled and organized by Projekt DEAL.

Conflict of Interest

The authors declare no conflict of interest.

Data Availability Statement

The data that support the findings of this study are available in the supplementary material of this article.

Keywords: Main Group Chemistry · Pentafluorosulfanyl · Propellane · Strained Molecules · X-Ray Diffraction

[1] a) S. Altomonte, M. Zanda, *J. Fluorine Chem.* **2012**, *143*, 57–93; b) P. R. Savoie, J. T. Welch, *Chem. Rev.* **2015**, *115*, 1130–1190; c) E. P. Gillis, K. J. Eastman, M. D. Hill, D. J. Donnelly,

N. A. Meanwell, *J. Med. Chem.* **2015**, *58*, 8315–8359; d) M. Sani, M. Zanda, *Synthesis* **2022**, *54*, 4184–4209; e) M. Magre, S. Ni, J. Cornella, *Angew. Chem. Int. Ed.* **2022**, *61*, e202200904; *Angew. Chem.* **2022**, *134*, e202200904.

[2] a) O. S. Kanishchev, W. R. Dolbier, in *Advances in Heterocyclic Chemistry, Vol. 120* (Eds.: E. F. V. Scriven, C. A. Ramsden), Academic Press, New York, **2016**, pp. 1–42; b) B. Cui, N. Shibata, *Phosphorus Sulfur Silicon Relat. Elem.* **2019**, *194*, 658–663; c) P. Beier, in *Emerging Fluorinated Motifs: Synthesis, Properties, and Applications, Vol. 2* (Eds.: J.-A. Ma, D. Cahard), Wiley-VCH, Weinheim, **2020**, pp. 551–570; d) G. Haufe, in *Emerging Fluorinated Motifs: Synthesis, Properties, and Applications, Vol. 2* (Eds.: J.-A. Ma, D. Cahard), Wiley-VCH, Weinheim, **2020**, pp. 571–609; e) R. Kordnezhadian, B.-Y. Li, A. Zogu, J. Demaerel, W. M. D. Borggraeve, E. Ismalaj, *Chem. Eur. J.* **2022**, *28*, e202201491.

[3] For some recent examples, see: a) D. J. Burton, Y. Wang, V. Bizet, D. Cahard, *e-EROS Encyclopedia of Reagents for Organic Synthesis*, Wiley, Chichester, **2001**; b) A. Gilbert, M. Birepinte, J.-F. Paquin, *J. Fluorine Chem.* **2021**, *243*, 109734–109743; c) G. Lefebvre, O. Charron, J. Cossy, C. Meyer, *Org. Lett.* **2021**, *23*, 5491–5495; d) V. Debrauwer, I. Leito, M. Lõkov, S. Tshepelevitsh, M. Parmentier, N. Blanchard, V. Bizet, *ACS Org. Inorg. Au* **2021**, *1*, 43–50; e) M. Birepinte, P. A. Champagne, J.-F. Paquin, *Angew. Chem. Int. Ed.* **2022**, *61*, e202112575; *Angew. Chem.* **2022**, *134*, e202112575.

[4] G. Haufe, *Tetrahedron* **2022**, *109*, 132656–132691.

[5] a) C. R. Pitts, D. Bornemann, P. Liebing, N. Santschi, A. Togni, *Angew. Chem. Int. Ed.* **2019**, *58*, 1950–1954; *Angew. Chem.* **2019**, *131*, 1970–1974; b) L. Wang, J. Cornella, *Angew. Chem. Int. Ed.* **2020**, *59*, 23510–23515; *Angew. Chem.* **2020**, *132*, 23716–23721; c) L. Wang, S. Ni, J. Cornella, *Synthesis* **2021**, *53*, 4308–4312.

[6] a) L. Zhong, P. R. Savoie, A. S. Filatov, J. T. Welch, *Angew. Chem. Int. Ed.* **2014**, *53*, 526–529; *Angew. Chem.* **2014**, *126*, 536–539; b) L. Zhong, A. S. Filatov, J. T. Welch, *J. Fluorine Chem.* **2014**, *167*, 192–197; c) P. Das, M. Takada, E. Tokunaga, N. Saito, N. Shibata, *Org. Chem. Front.* **2018**, *5*, 719–724.

[7] a) D. Bornemann, C. R. Pitts, C. J. Ziegler, E. Pietrasiak, N. Trapp, N. Santschi, A. Togni, *Angew. Chem. Int. Ed.* **2019**, *58*, 12604–12608; *Angew. Chem.* **2019**, *131*, 12734–12738; b) F. Brüning, C. R. Pitts, J. Kalim, D. Bornemann, C. Ghiazza, J. deMontmillon, N. Trapp, T. Billard, A. Togni, *Angew. Chem. Int. Ed.* **2019**, *58*, 18937–18941; *Angew. Chem.* **2019**, *131*, 19113–19117; c) J. Häfliger, C. R. Pitts, D. Bornemann, R. Käser, N. Santschi, J. Charpentier, E. Otth, N. Trapp, R. Verel, H. P. Lüthi, A. Togni, *Chem. Sci.* **2019**, *10*, 7251–7259; d) D. Bornemann, C. R. Pitts, L. Wettstein, F. Brüning, S. Küng, L. Guan, N. Trapp, H. Grützmacher, A. Togni, *Angew. Chem. Int. Ed.* **2020**, *59*, 22790–22795; *Angew. Chem.* **2020**, *132*, 22982–22988; e) D. Bornemann, F. Brüning, N. Bartalucci, L. Wettstein, C. R. Pitts, *Helv. Chim. Acta* **2021**, *104*, e2000218.

[8] C. R. Pitts, N. Santschi, A. Togni, WO2019229103, **2019**.

[9] J.-Y. Shou, X.-H. Xu, F.-L. Qing, *Angew. Chem. Int. Ed.* **2021**, *60*, 15271–15275; *Angew. Chem.* **2021**, *133*, 15399–15403.

[10] Y. Kraemer, E. N. Bergman, A. Togni, C. R. Pitts, *Angew. Chem. Int. Ed.* **2022**, *61*, e202205088; *Angew. Chem.* **2022**, *134*, e202205088.

[11] a) M. D. Levin, P. Kaszynski, J. Michl, *Chem. Rev.* **2000**, *100*, 169–234; b) W. Wu, J. Gu, J. Song, S. Shaik, P. C. Hiberty, *Angew. Chem. Int. Ed.* **2009**, *48*, 1407–1410; *Angew. Chem.* **2009**, *121*, 1435–1438; c) S. Shaik, D. Danovich, W. Wu, P. C. Hiberty, *Nat. Chem.* **2009**, *1*, 443–449; d) A. J. Sterling, A. B. Dürr, R. C. Smith, E. A. Anderson, F. Duarte, *Chem. Sci.* **2020**, *11*, 4895–4903.

[12] a) J. M. Lopchuk, K. Fjelbye, Y. Kawamata, L. R. Malins, C.-M. Pan, R. Gianatassio, J. Wang, L. Prieto, J. Bradow, T. A. Brandt, M. R. Collins, J. Elleraas, J. Ewanicki, W. Farrell, O. O. Fadeyi, G. M. Gallego, J. J. Mousseau, R. Oliver, N. W. Sach, J. K. Smith, J. E. Spangler, H. Zhu, J. Zhu, P. S. Baran, *J. Am. Chem. Soc.* **2017**, *139*, 3209–3226; b) F.-S. He, S. Xie, Y. Yao, J. Wu, *Chin. Chem. Lett.* **2020**, *31*, 3065–3072; c) J. Turkowska, J. Durka, D. Gryko, *Chem. Commun.* **2020**, *56*, 5718–5734.

[13] a) A. F. Stepan, C. Subramanyam, I. V. Efremov, J. K. Dutra, T. J. O'Sullivan, K. J. DiRico, W. S. McDonald, A. Won, P. H. Dorff, C. E. Nolan, S. L. Becker, L. R. Pustilnik, D. R. Riddell, G. W. Kauffman, B. L. Kormos, L. Zhang, Y. Lu, S. H. Capetta, M. E. Green, K. Karki, E. Sibley, K. P. Atchison, A. J. Hallgren, C. E. Oborski, A. E. Robshaw, B. Sneed, C. J. O'Donnell, *J. Med. Chem.* **2012**, *55*, 3414–3424; b) G. M. Locke, S. S. R. Bernhard, M. O. Senge, *Chem. Eur. J.* **2019**, *25*, 4590–4647; c) P. K. Mykhailiuk, *Org. Biomol. Chem.* **2019**, *17*, 2839–2849; d) E. G. Tse, S. D. Houston, C. M. Williams, G. P. Savage, L. M. Rendina, I. Hallyburton, M. Anderson, R. Sharma, G. S. Walker, R. S. Obach, M. H. Todd, *J. Med. Chem.* **2020**, *63*, 11585–11601.

[14] a) B. Stump, C. Eberle, W. B. Schweizer, M. Kaiser, R. Brun, R. L. Krauth-Siegel, D. Lentz, F. Diederich, *ChemBioChem* **2009**, *10*, 79–83; b) P. Wipf, T. Mo, S. J. Geib, D. Caridha, G. S. Dow, L. Gerena, N. Roncal, E. E. Milner, *Org. Biomol. Chem.* **2009**, *7*, 4163–4165; c) S. Altomonte, G. L. Baillie, R. A. Ross, J. Riley, M. Zanda, *RSC Adv.* **2014**, *4*, 20164–20176; d) M. V. Westphal, B. T. Wolfstädter, J.-M. Plancher, J. Gatfield, E. M. Carreira, *ChemMedChem* **2015**, *10*, 461–469; e) M. F. Sowaileh, R. A. Hazlitt, D. A. Colby, *ChemMedChem* **2017**, *12*, 1481–1490.

[15] a) C. Ramireddy, V. S. Reddy, P. Munk, C. N. Wu, *Macromolecules* **1991**, *24*, 1387–1391; b) M. Bremer, P. Kirsch, M. Klasen-Memmer, K. Tarumi, *Angew. Chem. Int. Ed.* **2013**, *52*, 8880–8896; *Angew. Chem.* **2013**, *125*, 9048–9065.

[16] S. Aït-Mohand, W. R. Dolbier Jr., *Org. Lett.* **2002**, *4*, 3013–3015.

[17] The complete details of our optimization and isolation can be found in the Supporting Information.

[18] a) J. R. Case, N. H. Ray, H. L. Roberts, *J. Chem. Soc.* **1961**, 2066–2070; b) J. R. Case, N. H. Ray, H. L. Roberts, *J. Chem. Soc.* **1961**, 2070–2075; c) H. W. Sidebottom, J. M. Tedder, J. C. Walton, *Trans. Faraday Soc.* **1969**, *65*, 2103–2109; d) R. E. Banks, R. N. Haszeldine, W. D. Morton, *J. Chem. Soc. C* **1969**, 1947–1949; e) T. Krügerke, K. Seppelt, *J. Fluorine Chem.* **1985**, *29*, 65; f) W. R. Dolbier Jr., S. Aït-Mohand, T. D. Schertz, T. A. Sergeeva, J. A. Cradlebaugh, A. Mitani, G. L. Gard, R. W. Winter, J. S. Thrasher, *J. Fluorine Chem.* **2006**, *127*, 1302–1310.

[19] a) W. D. Stohrer, R. Hoffmann, *J. Am. Chem. Soc.* **1972**, *94*, 779–786; b) K. B. Wiberg, S. T. Waddell, *J. Am. Chem. Soc.* **1990**, *112*, 2194–2216; c) Z. Wu, Y. Xu, J. Liu, X. Wu, C. Zhu, *Sci. China Chem.* **2020**, *63*, 1025–1029.

[20] For instance, see: a) K. B. Wiberg, S. T. Waddell, K. Laidig, *Tetrahedron Lett.* **1986**, *27*, 1553–1556; b) D. F. J. Caputo, C. Arroniz, A. B. Dürr, J. J. Mousseau, A. F. Stepan, S. J. Mansfield, E. A. Anderson, *Chem. Sci.* **2018**, *9*, 5295–5300; c) R. M. Bär, G. Heinrich, M. Nieger, O. Fuhr, S. Bräse, *Beilstein J. Org. Chem.* **2019**, *15*, 1172–1180.

[21] The distances reported for compound **2** throughout the manuscript are not corrected for libration. The libration corrected values appear in the Supporting Information.

[22] J. L. Adcock, A. A. Gakh, J. L. Pollitte, C. Woods, *J. Am. Chem. Soc.* **1992**, *114*, 3980–3981.

[23] a) J. F. Chiang, S. H. Bauer, *J. Am. Chem. Soc.* **1970**, *92*, 1614–1617; b) A. Almenningen, B. Andersen, B. A. Nyhus, *Acta Chem. Scand.* **1971**, *25*, 1217–1223.

[24] a) R. Bianchi, G. Morosi, A. Mugnoli, M. Simonetta, *Acta Crystallogr. Sect. B* **1973**, *29*, 1196–1208; b) J. Chandrasekhar, *Curr. Sci.* **1992**, *63*, 114–116.
[25] P. Liebing, C. R. Pitts, M. Reimann, N. Trapp, D. Rombach, D. Bornemann, M. Kaupp, A. Togni, *Chem. Eur. J.* **2021**, *27*, 6086–6093.
[26] a) P. Das, K. Niina, T. Hiromura, E. Tokunaga, N. Saito, N. Shibata, *Chem. Sci.* **2018**, *9*, 4931–4936; b) K. Maruno, K. Niina, O. Nagata, N. Sibata, *Org. Lett.* **2022**, *24*, 1722–1726; c) K. Iwaki, K. Maruno, O. Nagata, N. Shibata, *J. Org. Chem.* **2022**, *87*, 6302–6311; d) K. Iwaki, K. Tanagawa, S. Mori, K. Maruno, Y. Sumii, O. Nagata, N. Shibata, *Org. Lett.* **2022**, *24*, 3347–3352; e) K. Maruno, K. Hada, Y. Sumii, O. Nagata, N. Shibata, *Org. Lett.* **2022**, *24*, 3755–3759.
[27] P. Kaszynski, J. Michl, *J. Am. Chem. Soc.* **1988**, *110*, 5225–5226.
[28] K. Niina, K. Tanagawa, Y. Sumii, N. Saito, N. Shibata, *Org. Chem. Front.* **2020**, *7*, 1276–1282.
[29] B. Braïda, P. C. Hiberty, *Nat. Chem.* **2013**, *5*, 417–422.
[30] D. D. Davis, R. H. Black, *J. Organomet. Chem.* **1974**, *82*, C30–C34.
[31] a) K. B. Wiberg, V. Z. Williams Jr., *J. Am. Chem. Soc.* **1967**, *89*, 3373–3374; b) A. Padwa, E. Shefter, E. Alexander, *J. Am. Chem. Soc.* **1968**, *90*, 3717–3721; c) K. B. Wiberg, C. M. Hadad, S. Sieber, P. V. R. Schleyer, *J. Am. Chem. Soc.* **1992**, *114*, 5820–5828; d) K. B. Wiberg, N. McMurdie, *J. Am. Chem. Soc.* **1994**, *116*, 11990–11998; e) J. H. Kim, A. Ruffoni, Y. S. S. Al-Faiyz, N. S. Sheikh, D. Leonori, *Angew. Chem. Int. Ed.* **2020**, *59*, 8225–8231; *Angew. Chem.* **2020**, *132*, 8302–8308; f) J. M. Anderson, N. D. Measom, J. A. Murphy, D. L. Poole, *Angew. Chem. Int. Ed.* **2021**, *60*, 24754–24769; *Angew. Chem.* **2021**, *133*, 24958–24973.
[32] a) E. W. Della, C. H. Schiesser, *J. Chem. Soc. Chem. Commun.* **1994**, 417–419; b) W. Adcock, A. R. Krstic, *Magn. Reson. Chem.* **2000**, *38*, 115–122.
[33] J. I. Wu, P. V. R. Schleyer, *Pure Appl. Chem.* **2013**, *85*, 921–940.
[34] Gaussian 09, Revision D.01; Gaussian, Inc.: Wallingford, CT, **2013**.
[35] K. B. Wiberg, *Tetrahedron* **1968**, *24*, 1083–1096.
[36] I. V. Alabugin, G. dos Passos Gomes, M. A. Abdo, *WIREs Comput. Mol. Sci.* **2019**, *9*, e1389.
[37] T. Laube, *Acc. Chem. Res.* **1995**, *28*, 399–405.
[38] K. B. Wiberg, *Tetrahedron Lett.* **1985**, *26*, 599–602.
[39] Deposition Numbers 2195538, 2195539, 2195540, 2195541, 2195782, 2195783, 2195784, 2195785, and 2195786 contain the supplementary crystallographic data for this paper. These data are provided free of charge by the joint Cambridge Crystallographic Data Centre and Fachinformationszentrum Karlsruhe Access Structures service.

Manuscript received: August 11, 2022
Accepted manuscript online: September 22, 2022
Version of record online: October 25, 2022